Friction and Wear of Al_2O_3-Based Composites with Dispersed and Agglomerated Nanoparticles

Jinjun Lu, Jian Shang, Junhu Meng and Tao Wang

Abstract In recent years, Al_2O_3-based nanocomposite which is composed of micro-size Al_2O_3 matrix and a second phase nanoparticles (e.g. SiC, Ni) as the reinforcement phase have received considerable attention and come a long way mainly because of their good mechanical property and resistance to abrasive wear and erosive wear. Up to now, practice on tribologcial design and testing of high temperature self-lubricating Al_2O_3-based nanocomposites is an exciting field to be explored. In this chapter, the principle for fabrication of Al_2O_3-based nanocomposite for better mechanical property than that of monolithic Al_2O_3 ceramic is briefly introduced on basis of literature review. In other words, the microstructure, and mechanical property of Al_2O_3-SiC, Al_2O_3-Ni nanocomposites are briefly introduced and discussed. This chapter focuses on the design and tribological property of high temperature self-lubricating Al_2O_3-based nanocomposites. As the first step, the tribological consideration of Al_2O_3-SiC nanocomposite is discussed according to Todd's work which gives useful information on the pullouts of grains during grinding and polishing. In addition, a concept for designing high temperature self-lubricating Al_2O_3-based nanocomposite with dispersed and agglomerated ceramic nanoparticles is proposed and discussed using Al_2O_3-TiCN composite as an example. Al_2O_3-5 wt % TiCN and Al_2O_3-10 wt % TiCN composites had high hardness and good tribological property at room temperature in air. Al_2O_3-TiCN composites containing 10 wt % and 20 wt % TiCN nanoparticles in sliding against Ni-Cr alloy are self-lubricating at 500 °C.

J. Lu (✉) · J. Shang · J. Meng · T. Wang
State Key Laboratory of Solid Lubrication, Lanzhou Institute of Chemical Physics,
Chinese Academy of Sciences, 730000 Lanzhou, China
e-mail: jjlu@licp.cas.cn

J. Paulo Davim (ed.), *Tribology of Nanocomposites*, Materials Forming, Machining and Tribology, DOI: 10.1007/978-3-642-33882-3_4,

1 Introduction

Alumina (Al_2O_3) is one of the five important classes of advanced structural ceramics. In addition, ceramics based on Al_2O_3 have been used in commercial applications for many years because of their availability and low cost [1]. There are many efforts to improve the mechanical and tribological property of Al_2O_3 ceramic by adding a second phase particles. The particles are mostly micro-size particles.

In the 1990s, the concept of Al_2O_3-based nanocomposite was proposed and two representatives of this kind of nanocomposites, i.e. Al_2O_3-SiC and Al_2O_3-Ni, have been successfully fabricated. The mechanical property of this kind of nanocomposite is very appealing. For specification, some of the reported bending strengths of the two nanocomposites are as high as 1 GPa which is much higher than that of monolithic Al_2O_3 ceramic [2, 3]. This result has driven many researchers to reveal the strengthening mechanism of SiC and Ni nanoparticles. Despite their very high bending strength, the fracture toughness of Al_2O_3-SiC and Al_2O_3-Ni nanocomposites is not high enough to make them a tough material. The discussion will be forwarded later in Sect. 1.1.2.

In this section, the principle for fabrication of Al_2O_3-based nanocomposite for better mechanical property than that of monolithic Al_2O_3 ceramic is introduced on basis of literature review. To specify, the microstructure, mechanical property and tribological property of Al_2O_3-based nanocomposite will be introduced and discussed.

1.1 Microstructure, Mechanical and Tribological Property of Al_2O_3-Based Nanocomposite

1.1.1 Microstructure

The main weakness of monolithic Al_2O_3 ceramic as a structural material is its intrinsic brittleness. To make Al_2O_3 ceramic tougher, a second phase in form of particle, whisker, and fiber is often added. The micro-size particle, whisker, and fiber can indeed increase the fracture toughness of Al_2O_3 ceramic [2]; however, the sacrifice of strength is the drawback of this kind of toughening mechanism.

In the 1990s, a new concept is proposed to solve the above problem. The microstructure of Al_2O_3-based nanocomposite can be classified into two groups: micro-size Al_2O_3 matrix with nano-size particle or whisker (group I) and nano-size Al_2O_3 matrix with nano-size particle or whisker (group II). The group I can be further divided into three subgroups according to the location of nano-size particle or whisker. The three subgroups are inter-type, intra-type and inter/intra-type. Up to now, Al_2O_3-based nanocomposite in the published papers belongs to group I. In the following section, unless otherwise stated, Al_2O_3-based nanocomposite refers to Al_2O_3-based nanocomposite of group I. Al_2O_3-based nanocomposite of group II is expected to have several attractive functions, e.g. superplasticity and good machinability but is still an myth now. The type of Al_2O_3-based nanocomposite is summarized in Table 1.

Table 1 Type of Al_2O_3-based nanocomposite

Group	Sub-Group	Description
I. Micro-nano type	Inter-type Intra-type Inter/intra-type	Micro-size Al_2O_3 matrix, submicro-size or nano size second phase particles
II. Nano-nano type		Nano-size Al_2O_3 matrix, nano-size second phase particles

The second phase particles for Al_2O_3-based nanocomposite in Table 1 are generally required to be well dispersed rather than agglomerated. However, the agglomerated nanoparticles are sometimes useful from viewpoint of tribology and will be discussed later.

1.1.2 Mechanical Property

The addition of nano-size particle or whisker in Al_2O_3-based nanocomposite has at least two beneficial effects on mechanical property. One is the fine grain Al_2O_3 matrix and the other is the pinning effect of nano-size particle or whisker.

The initial aim for preparing Al_2O_3-based nanocomposite is to increase the fracture toughness. According to the published data, the increment in fracture toughness is very limited. On the other hand, it is very interesting that the three-point bending strength of Al_2O_3-based nanocomposite is high up to 1 GPa. The high bending strength indicates that Al_2O_3-based nanocomposite is capable of tolerating high tensile stress while the limited improvement on fracture toughness indicates Al_2O_3-based nanocomposite is still a brittle material.

It is convincing to elucidate the high bending strength of Al_2O_3-based nanocomposite from Todd's work [4–6]. As it will be shown in the next section, the area fraction of pullout of grains and pullout diameter on the surface of Al_2O_3-based nanocomposite are lower than that of monolithic Al_2O_3 ceramic. As a consequence, the number and size of the defects on a beam made of Al_2O_3-based nanocomposite for a three-point bending test are lower than that on a beam made of monolithic Al_2O_3 ceramic. It is the defect (pullout of grain) that determines the difference in bending strength of Al_2O_3-based nanocomposite and monolithic Al_2O_3 ceramic. The contribution of reducing pullout of grains to the fracture toughness is limited.

1.1.3 Tribological Property

Findings indicate that Al_2O_3-based nanocomposite exhibits better tribological performance than that of monolithic Al_2O_3 ceramic [7, 8]. Of these tribological investigations, the tribological property of Al_2O_3-based nanocomposite is mainly on friction and wear dominated by fracture and pullout of grains, e.g. abrasive wear and erosive wear.

The abrasive wear of Al_2O_3-SiC nanocomposite is systematically investigated by Todd and his main contribution to this field is the discovery of quantity and type of pullout of grains. He uses two parameters, area fraction of pullout and pullout diameter, for comparison of the wears of Al_2O_3-SiC nanocomposite and monolithic Al_2O_3 ceramic. The area fraction of pullout and pullout diameter for Al_2O_3-SiC nanocomposite are lower than that of monolithic Al_2O_3 ceramic. The fraction of transgranular and intergranular pullout is also useful for understanding the wear mechanism. The results of abrasive wear of Al_2O_3-SiC nanocomposite is very helpful for the understanding of high three-point bending strength mentioned in Sect. 1.1.2. The surface defects on the beam of Al_2O_3-SiC nanocomposite for a three-point bending test are mainly pullout of grain and the number of surface defects can be greatly reduced during the grinding and polishing.

Fine grain and less number of surface defect are also very useful for good wear resistance for erosive wear. In this sense, the wear resistance of Al_2O_3-SiC nanocomposite to erosive wear is good.

1.2 Tribological Consideration of High Temperature Self-Lubricating Al_2O_3-Based Nanocomposite

Up to now, the tribological properties of Al_2O_3-SiC and Al_2O_3-Ni nanocomposites including sliding friction and wear as well as abrasive wear have been evaluated. And some results are quite good indeed.

However, as is known to the readers, the basis principle for designing these Al_2O_3-based nanocomposite is based on the viewpoint of improving the mechanical strength, not the tribological property. The principles for fabrication of a structural material and a tribo-material are common and uncommon in many aspects. There are two examples. The first one is about the common aspect. Fine grain Al_2O_3 matrix is preferred for improving mechanical and tribological properties. The second one is about the uncommon aspect. The second phase particles in Al_2O_3-based nanocomposite can be well dispersed and agglomerated for good tribological behavior but only well dispersed for good mechanical property. That is to say, an optimized microstructure of an Al_2O_3-based nanocomposite for high mechanical strength might not be an optimized one for low friction and/or high wear resistance. Therefore, it is urgent to propose material design from the viewpoint of tribology.

In this chapter, we propose a concept which is derived from the concept in Table 1, to design high temperature self-lubricating Al_2O_3-based nanocomposite. The proposed high temperature self-lubricating Al_2O_3-based nanocomposite is composed of a micro-size Al_2O_3 matrix and a second phase nanoparticle. The second phase nanoparticle should be served as both strengthening component and tribological component. In this sense, some solid lubricants, e.g. MoS_2, graphite, CuO, PbO, are not qualified as strengthening component. Ni, Cu and Mo are a

good choice because they can improve the bending strength. In addition, the oxides of Ni, Cu and Mo are lubricious at high temperature. The two points can make Al_2O_3-Ni (Cu, W) nanocomposite as high temperature self-lubricating materials. Another group of the second phase nanoparticle contains hard carbides (e.g. SiC, TiC, WC, TiCN) and borides (e.g. TiB_2). These carbides and borides have high melting point and hardness and can strengthen Al_2O_3 ceramic. The nanoparticles of carbides and borides can be readily oxidized at high temperature and the oxides are lubricious. Besides dispersed nanoparticles, agglomerated nanoparticles might be helpful for the formation of continuous lubricious oxide film on the worn surface.

In summary, the basic points of the concept are: (1) Fine grain Al_2O_3 matrix with typical grain size of less than 3 μm. (2) The second phase nanoparticles can strengthen Al_2O_3 ceramic. (3) Lubrication is provided by lubricious oxide generated by tribo-oxidation of nanoparticles at high temperature. (4) Agglomerated nanoparticles give birth to continuous lubricious oxide film on the worn surface.

The tribological behaviors of a Ni-based alloy/Al_2O_3 tribo-pair at elevated temperatures are of theoretical importance. The dominate wear mechanism of a metal/Al_2O_3 tribo-pair at high temperature is adhesive wear which is evident by severe material transfer from alloy to Al_2O_3. Some oxides (e.g. CuO) and tribo-oxides (TiO_2 from TiCN, TiC) can eliminate or prevent the material transfer from Ni-based alloy to Al_2O_3 and reducing the friction coefficient. TiCN has a high hardness comparable to SiC and can be used as a second phase for improving the mechanical strength of Al_2O_3. The tribo-oxide of TiCN at high speed and elevated temperatures can provide effective lubrication on the frictional surface of Al_2O_3. This means TiCN can be used as both strengthening component and tribological component for Al_2O_3. From the viewpoint of sintering, the sintering temperature of TiCN is higher than that of Al_2O_3 and this enables the dispersed and agglomerated TiCN nanoparticles in the Al_2O_3 matrix. In this connection, Al_2O_3-TiCN composite with dispersed and agglomerated nanoparticles is used as an example of this chapter. In the following sections, the preparation, microstructure, mechanical property and tribological property of Al_2O_3-TiCN composite will be introduced.

2 Preparation, Microstructure and Mechanical Property of Al_2O_3-TiCN Composite

2.1 Material

2.1.1 Preparation

Al_2O_3 and $Ti(C_{0.3}N_{0.7})$ powders to fabricate Al_2O_3-TiCN composite were commercially available from Nanjing Emperor Nano Material Co., Ltd. and Shijiazhuang Huatai Nanoceramic Factory. The average particle sizes of Al_2O_3 and $Ti(C_{0.3}N_{0.7})$ powders are 0.5 μm and 50 nm, respectively.

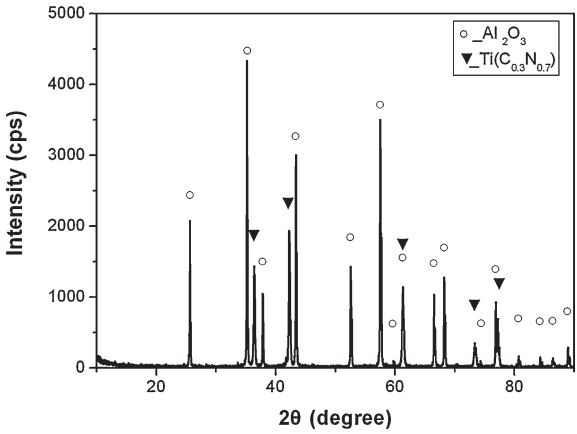

Fig. 1 The XRD pattern of A10T composite

Al_2O_3 and $Ti(C_{0.3}N_{0.7})$ powders were mechanically mixed in a HF-G7-R75S2 Planetary Grinding Machine (Nanjing NanDa Instrument Plant, China) using agate balls and alcohol as grinding media. The weight ratio of ball and powder was 10:1. Composite powders with mass fractions of 5, 10, 20, 30, and 40 % for $Ti(C_{0.3}N_{0.7})$ were prepared to fabricate corresponding Al_2O_3-TiCN composites. In the following section, A5T, A10T, A20T, A30T and A40T are abbreviations for Al_2O_3-TiCN composites with mass fractions of 5, 10, 20, 30, and 40 % of $Ti(C_{0.3}N_{0.7})$.

One-step sintering was used to fabricate Al_2O_3-TiCN composite. The mixed Al_2O_3-$Ti(C_{0.3}N_{0.7})$ powders were hot pressed in a graphite die using a ZT-63-20Y vacuum hot-pressing sintering furnace (manufactured by Shanghai Chen Hua Electric Furnace Co. Ltd.). The hot pressing was conducted at a sintering temperature of 1,400 °C and a pressure of 30 MPa for 120 min in Ar gas. The sintering parameters was optimized for monolithic Al_2O_3 ceramic, not for Al_2O_3-TiCN composites in this chapter. Moreover, a sintering temperature of 1,400 °C is not high enough for sintering and apparent grain growth of TiCN particles. As a result, it is important that TiCN particles remain as nanoparticles in the composite. In addition, the agglomerated TiCN nanoparticles in Al_2O_3-TiCN composite can be achieved by adding adequate amount of TiCN particles.

2.1.2 Microstructure and Mechanical Property

The microstructure of Al_2O_3-TiCN composites was investigated using X-ray diffraction (XRD) to determine the phase composition and scanning electron microscopy (SEM) to determine the grain sizes of Al_2O_3 and TiCN and distribution of TiCN particles.

XRD results show that all the Al_2O_3-TiCN composites were composed of two phases, i.e. α-Al_2O_3 and TiCN; no chemical reaction between Al_2O_3 and TiCN and no decomposition of TiCN occurred, see Fig. 1.

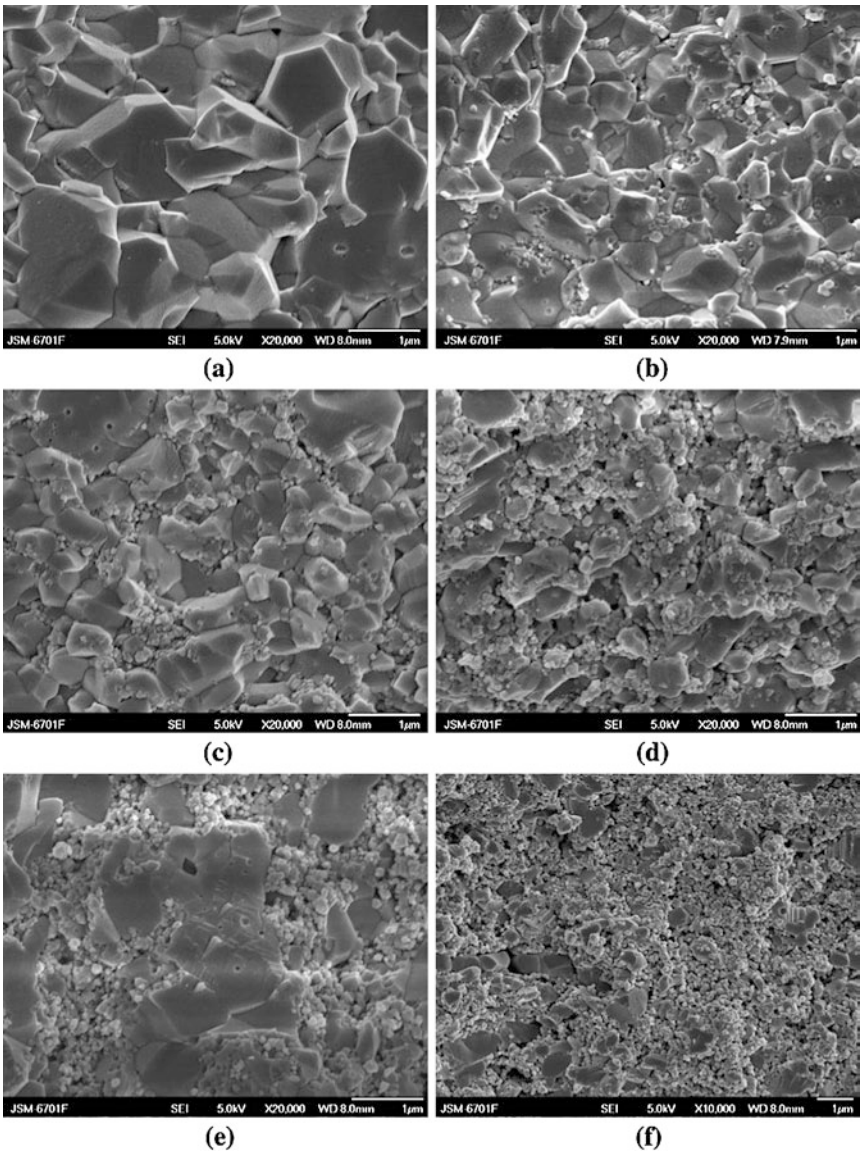

Fig. 2 SEM micrographs of fractured surface of monolithic Al_2O_3 ceramic and Al_2O_3-TiCN composites. The mass fractions of TiCN are **a** 0 %, **b** 5 %, **c** 10 %, **d** 20 %, **e** 30 %, **f** 40 %

Monolithic Al_2O_3 ceramic in Fig. 2a had a dense and fine grain microstructure. The average grain size d50 was 3 μm. As seen in Fig. 2, by varying the addition amount of TiCN nanoparticles, the Al_2O_3-TiCN composites exhibited evolution of microstructures in some aspects, i.e. the grain size and distribution of Al_2O_3; distribution of TiCN nanoparticles; agglomeration of TiCN nanoparticles.

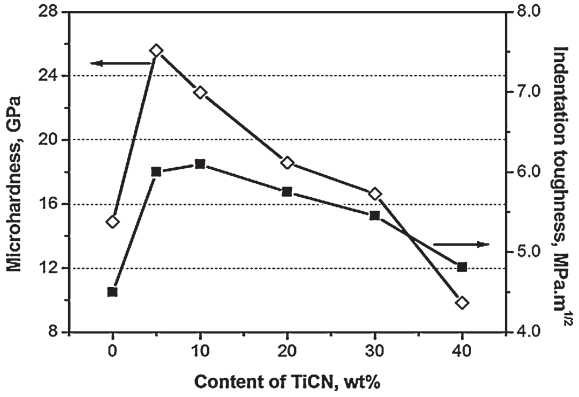

Fig. 3 Microhardness and indentation toughness of the Al_2O_3-TiCN composites

In general, the incorporation of TiCN nanoparticles inhibited the growth of Al_2O_3 grain and thereby reduced the grain size of Al_2O_3 at the same sintering temperature. The grain sizes of Al_2O_3 in Fig. 2b to 2f were smaller than that in Fig. 2a. The addition of 5 wt % TiCN nanoparticles can effectively reduce the grain size of Al_2O_3 to ca. 1 μm, see Fig. 2b. Higher addition amount of TiCN nanoparticles, i.e. 10 wt % and more, can reduce the grain size of Al_2O_3; however, some large Al_2O_3 grains can also be found, see Fig. 3e. Al_2O_3 was considered as the matrix in Fig. 2b to d but was separated by agglomerated TiCN nanoparticles in Fig. 2e and f.

For A5T composite, the distribution of TiCN nanoparticles in Al_2O_3 matrix was not even with very small fraction of agglomerated TiCN nanoparticles; and both inter-type and intra-type TiCN nanoparticles can be found. In this chapter, the relative amount of inter-type and intra-type TiCN nanoparticles was not determined. A10T composite had a similar microstructure as that of A5T composite comparing Figs. 2b and 2c.

The degree of agglomeration of TiCN nanoparticles transited at an addition amount of 20 wt % and became severe at an addition amount of 40 wt %. For the five Al_2O_3-TiCN composites, the maximum size of TiCN nanoparticle was lower than 150 nm.

In summary, the Al_2O_3-TiCN composites with 5 and 10 wt % TiCN had well-dispersed TiCN nanoparticles and A20T, A30T and A40T composites had agglomerated TiCN nanoparticles.

The microhardness and indentation toughness of A5T and A10T composites were higher than that of monolithic Al_2O_3 ceramic. This indicates the two composites had good mechanical property, see Fig. 3. The microhardness of Al_2O_3-TiCN composites with higher mass fraction of TiCN were lower than 20 GPa and not considered as materials with good mechanical property.

In summary, A5T and A10T composites had good microstructure for good mechanical property. The mechanical property of A20T composite might be improved by optimizing the sintering parameters.

3 Tribological Property and Wear Mechanism of Al_2O_3-TiCN Composite

3.1 Experimental

3.1.1 Tribological Tests

Tribological tests were conducted on a THT high temperature tribometer (CSM Instrument Ltd., Switzerland) with a pin-on-disk configuration at room temperature and 500 °C in air. Friction coefficient was automatically recorded by the computer. The test condition is 5 N for normal load and 0.5 m/s for sliding speed and 1 km for sliding distance. The contact between the hemispherical tip of the pin and the flat surface of the disk is believed to be stable and enables good repeatability of the test.

The pin was made of a Ni-20 wt % Cr alloy (Ni-Cr alloy) prepared by hot pressing at 1,200 °C and 15 MPa for 15 min. The Ni-Cr alloy pin had a size of 6 mm in diameter and 12 mm in length. One end of the pin was machined into a hemispherical tip with a radius of 6 mm for the sliding contact. The surface roughness Ra of the ground hemispherical tip was lower than 0.3 μm. The disk was made of monolithic Al_2O_3 ceramic or Al_2O_3-TiCN composite with a size of 25 mm in diameter and 8 mm in thickness. The surface roughness Ra of the polished disk was lower than 0.1 μm. Both the pin and disk were ultrasonically cleaned in an ethanol bath and allowed to dry prior to the tribological test.

The wear volume of the pin was determined by measuring the wear scar diameter of the pin. The 3D topography of the worn surface of monolithic Al_2O_3 ceramic and Al_2O_3-TiCN composite was observed on a Micro XAM Interferometric Surface Profile (ADE, USA). The wear volume and surface profile of the cross-sectioned wear scar of the disk can be obtained accordingly.

3.1.2 Characterization of Worn Surface

The morphology of the worn surface of monolithic Al_2O_3 ceramic and Al_2O_3-TiCN composite was observed on a SEM (JSM 5600LV, Japan) using secondary electron image (SEI) and backscattered electron image (BEI). The chemical state of typical elements on the worn surface of monolithic Al_2O_3 ceramic and Al_2O_3-TiCN composite was determined by X-ray Photoelectron Spectroscopy (XPS, PHI-5702, USA).

3.2 Results

3.2.1 Tribological Behavior

Room temperature. Friction coefficients of monolithic Al_2O_3 ceramic and Al_2O_3-TiCN composites in sliding against Ni–Cr alloy at room temperature were as high as around 0.7, see Fig. 4a. However, the wear rates of monolithic Al_2O_3 ceramic,

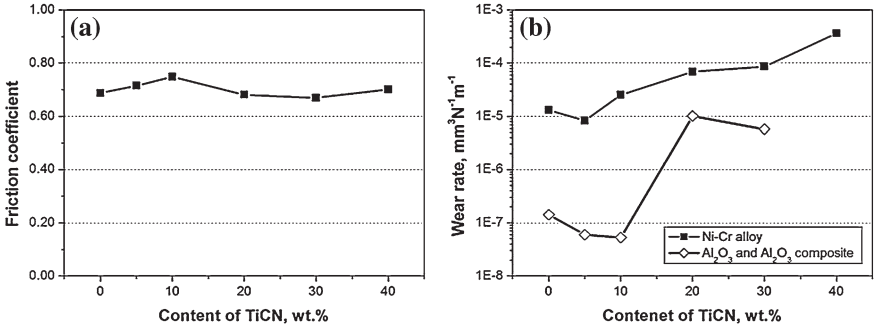

Fig. 4 **a** Friction coefficient and **b** wear rates of Al_2O_3-Ti(CN) composite in sliding against Ni-Cr alloy at room temperature in air. The wear rate of A40T composite is extremely high and not plotted in the figure

Al_2O_3-TiCN composites and their counterpart Ni-Cr alloy ranged from 10^{-8} to 10^{-4} $mm^3/(N.m)$, see Fig. 4b. In addition, the wear rates of monolithic Al_2O_3 ceramic and Al_2O_3-TiCN composites were much lower than that of corresponding Ni-Cr alloy. For example, the wear rates of monolithic Al_2O_3 ceramic and Ni-Cr alloy were on the order of magnitude of 10^{-7} $mm^3/(N.m)$ and 10^{-5} $mm^3/(N.m)$, respectively. Compared with monolithic Al_2O_3 ceramic, the wear rates of Al_2O_3-5 wt % TiCN composite and its counterpart material were lower. The wear rate of A10T composite was even lower but the wear rate of Ni-Cr alloy was higher. The wear resistances of Al_2O_3-TiCN composites (20 wt % and higher content of TiCN) and Ni-Cr alloy were very poor, especially for the composite.

High temperature at 500 °C. Friction coefficients of monolithic Al_2O_3 ceramic and Al_2O_3-TiCN composites in sliding against Ni-Cr alloy at 500 °C were lower than that at room temperature, i.e. 0.2 for A10T and A20T composite; 0.4 for the rest materials, see Fig. 5a. Therefore, the A10T and A20T composites were high temperature self-lubricating materials. The wear rates of Ni-Cr alloys in sliding against these two composites were on the order of magnitude of 10^{-7} to 10^{-6} $mm^3/(N.m)$ and lower than that against the rest materials, see Fig. 5b. Negative wear, which was the result of material transfer from Ni-Cr alloy, was found for monolithic Al_2O_3 ceramic and Al_2O_3-TiCN composites, see Fig. 5b. In addition, the absolute value of the negative wear is an indication of the amount of transferred material. It is interesting that the volume of the transferred material on A20T composite was about 10 times as high as that on A10T composite despite the two composites had identical friction coefficient.

The above results in Figs. 4 and 5 indicate that the tribological behaviors and wear mechanisms of monolithic Al_2O_3 ceramic and Al_2O_3-TiCN composites in sliding against Ni-Cr alloy depend on testing temperature and content of TiCN. As a good example, the frictional traces of A10T composite in sliding against Ni-Cr alloy at room temperature and 500 °C indicate different tribological

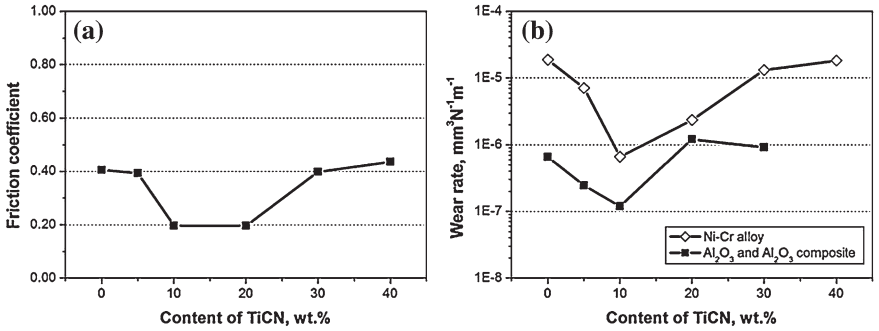

Fig. 5 **a** Friction coefficient and **b** wear rate of monolithic Al_2O_3 ceramic and Al_2O_3-Ti(CN) composite in sliding against Ni-Cr alloy at 500 °C in air. The wear rates of monolithic Al_2O_3 ceramic and Al_2O_3-TiCN composites were negative but presented in absolute value just for better reading

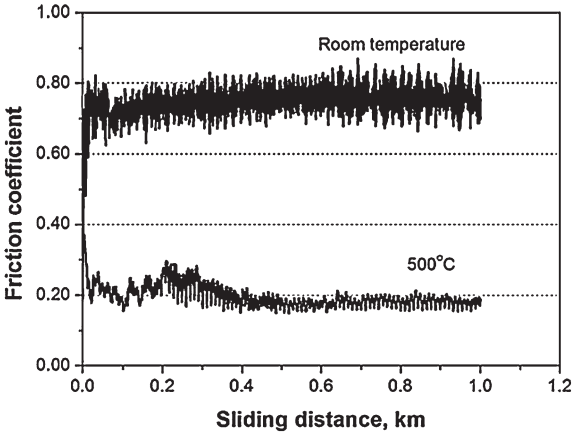

Fig. 6 Typical frictional traces of A10T composite in sliding against Ni-Cr alloy at room temperature and 500 °C

behavior, see Fig. 6. In the following section, the wear mechanisms at room temperature and 500 °C will be separately discussed.

3.2.2 Abrasive Wear and Transfer at Room Temperature

Abrasive wear and transfer (adhesive wear) were the two main wear mechanisms of monolithic Al_2O_3 ceramic and Al_2O_3-TiCN composites in sliding against Ni-Cr alloy at room temperature.

Abrasive wear can be clearly found by observing the 3D morphology and line profile of the wear tracks of monolithic Al_2O_3 ceramic and Al_2O_3-TiCN composites, see Fig. 7. The abrasive particles was generated from monolithic Al_2O_3 ceramic and Al_2O_3-TiCN composites. The resistances to abrasion of monolithic Al_2O_3 ceramic and Al_2O_3-TiCN composites (5 and 10 wt % TiCN) were excellent as evident by shallow scratch marks in Fig. 7a, a', b, b', c, and c'.

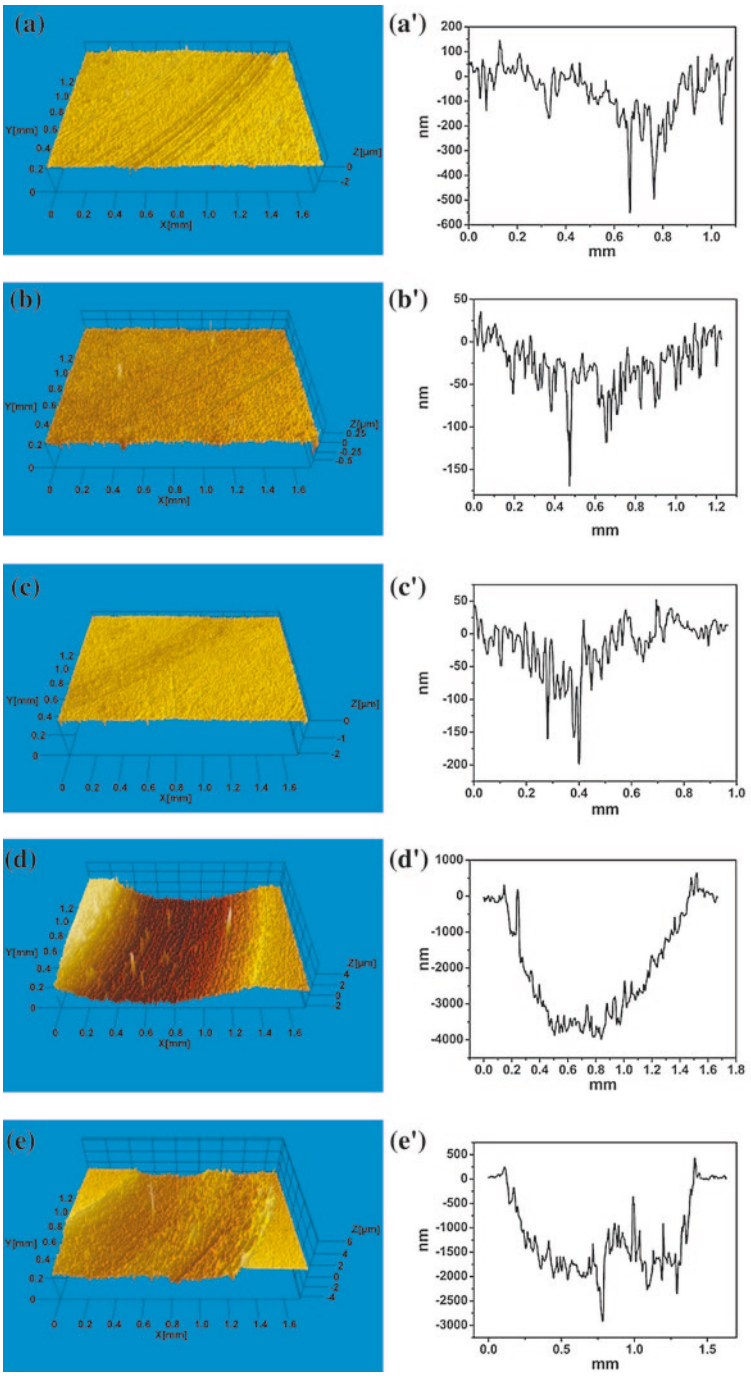

Fig. 7 3D morphologies of the wear tracks of **a** monolithic Al_2O_3 ceramic, **b** A5T composite, **c** A10T composite, **d** A20T composite, **e** A30T composite at room temperature and corresponding line profiles of **a**' monolithic Al_2O_3 ceramic, **b**' A5T composite, **c**' A10T composite, **d**' A20T composite, **e**' A30T composite

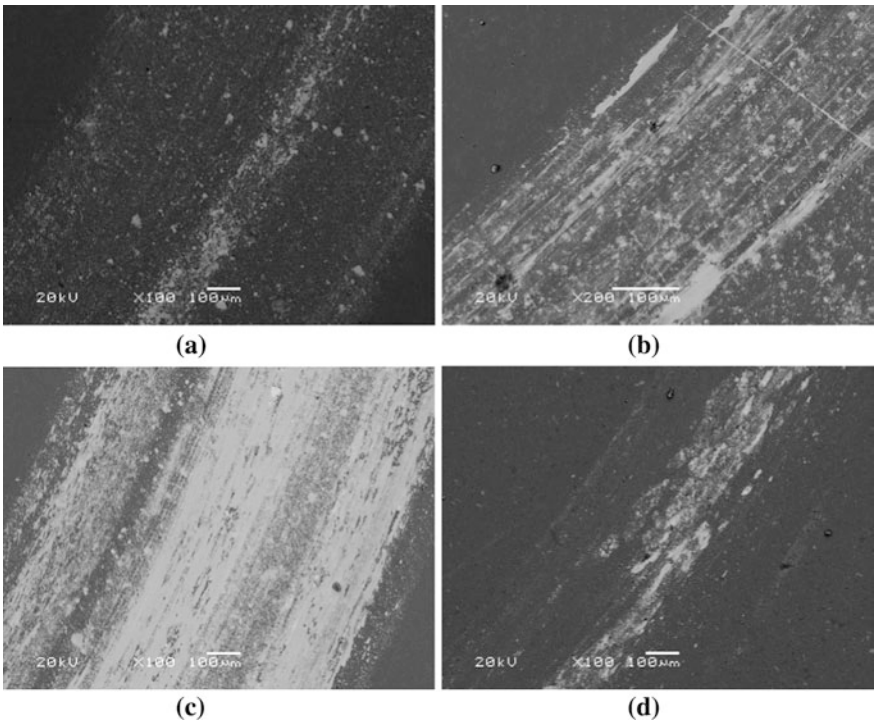

Fig. 8 BEI images of the worn surfaces of **a** monolithic Al_2O_3 ceramic and **b** A5T composite at room temperature and **c** monolithic Al_2O_3 ceramic and A10T composite at 500 °C. The transfer layer is located at the white area

The depth of the scratch mark on monolithic Al_2O_3 ceramic was 300 nm. Due to the reinforcement from hard TiCN nanoparticles in Al_2O_3 matrix, the depth of the scratch marks on A5T and A10T composites were 150 and 100 nm. The agglomerated TiCN nanoparticles in A20T composite (Fig. 2d) were easily pull out as abrasive particles and the resistance to abrasion of the composite was very poor, see Fig. 7d and d'. This is the same for A30T composite, see Fig. 7e and e'.

The transfer layers on monolithic Al_2O_3 ceramic and Al_2O_3-TiCN composites can be identified by BEI image (Fig. 8a). The transfer can be enhanced by the TiCN nanoparticles in Al_2O_3 matrix, see Fig. 8b.

3.2.3 Transfer and Tribo-Oxidation at 500 °C

For monolithic Al_2O_3 ceramic, transfer was greatly enhanced at 500 °C and obviously severer than that at room temperature, see Fig. 8c. The highest asperity on the worn surface of monolithic Al_2O_3 ceramic at 500 °C can be as high as 1.2 μm,

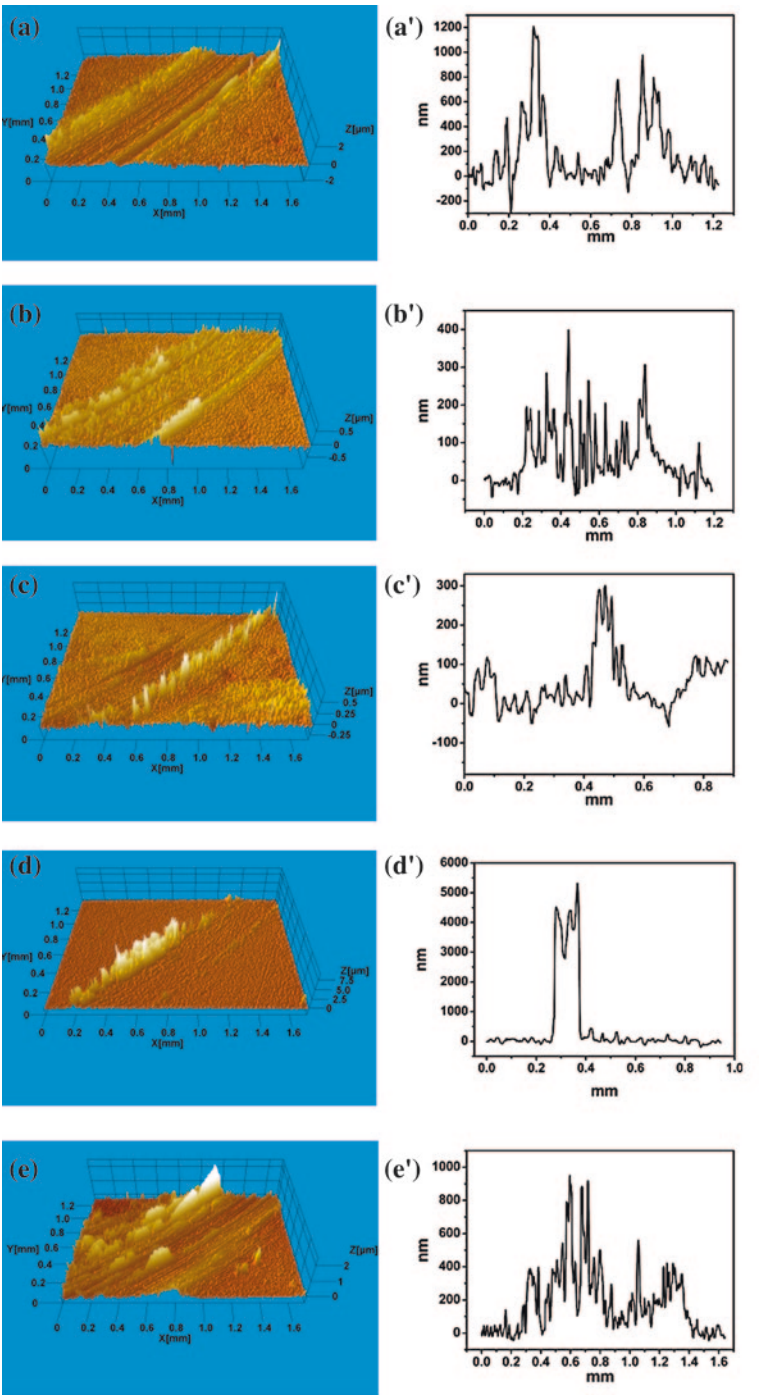

Fig. 9 3D morphologies of the wear tracks of **a** monolithic Al_2O_3 ceramic, **b** A5T composite, **c** A10T composite, **d** A20T composite, **e** A30T composite at 500 °C and corresponding line profiles of **a'** monolithic Al_2O_3 ceramic, **b**' A5T composite, **c**' A10T composite, **d**' A20T composite, **e**' A30T composite

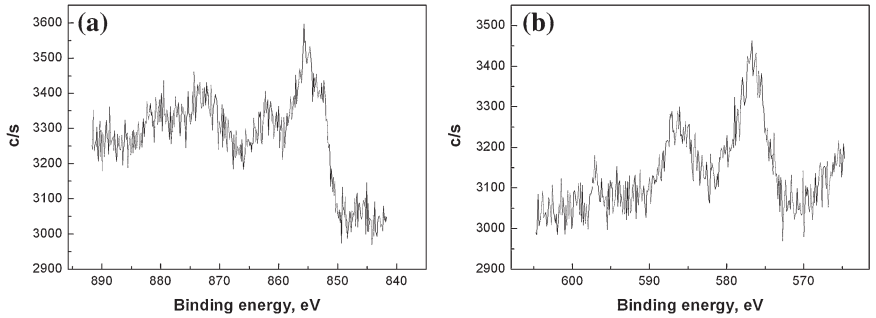

Fig. 10 XPS spectra of **a** Ni_2p, and **b** Cr_2p on the worn surface of monolithic Al_2O_3 ceramic at 500 °C

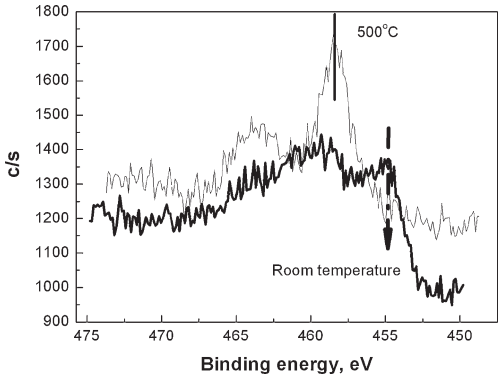

Fig. 11 XPS spectra of Ti_2p on the worn surface of A10T composite at room temperature and 500 °C in air

see Fig. 9a and a'. XPS spectra in Fig. 10 reveal that the transfer layer on monolithic Al_2O_3 ceramic at 500 °C was composed of Ni, NiO and Cr_2O_3. As such, the tribological contact was not a pure metal to metal contact, and NiO was responsible for the lower friction coefficient (0.4) than that (0.7) at room temperature.

According to Fig. 5b, the amount of transferred material on Al_2O_3-TiCN composites depended on the content of TiCN nanoparticles in the composite. Fig. 9 clearly demonstrates the transfer layer on the worn surfaces. It is interesting that A5T and A10T composites had small amount of transferred material but quite different friction coefficient. Meanwhile, A10T composite and A20T composite had quite different amount of transferred material but identical friction coefficient.

Tribo-oxidation of TiCN nanoparticles at 500 °C was the key to understand the above results. TiCN nanoparticles can be statically oxidized at 500 °C in air. The tribo-oxidation readily occurred at the sliding interface, see Fig. 11 and the tribo-product TiO_2, which is a softer oxide in comparison with Al_2O_3, modified the chemical composition and microstructure of the tribo-interface.

The tribo-interface modified by TiO_2 played important roles in preventing the transfer from Ni-Cr alloy and reducing friction coefficient at 500 °C. The tribo-oxidation of agglomerated TiCN nanoparticles in A20T composite took advantage over that of dispersed TiCN nanoparticles in A5T composite in friction reduction.

3.3 Discussion

In Sect. 3.2, the tribological behaviors of Al_2O_3-Ti(CN) composites with dispersed and agglomerated TiCN nanoparticles in sliding against Ni-Cr alloy at room temperature and 500 °C in air were investigated. At room temperature, dispersed TiCN nanoparticles in A5T composite and A10T composite made the composite harder and more wear resistant. Agglomerated TiCN nanoparticles (20, 30 and 40 wt % TiCN) were not good for mechanical property and wear resistance. Sintering temperature of these three composites might be not high enough for making a dense microstructure. The TiCN nanoparticles can be readily pullout and act as abrasive particles in the sliding interface.

Transfer was enhanced at 500 °C for monolithic Al_2O_3 ceramic in sliding against Ni-Cr alloy. Tribo-oxidation of dispersed TiCN nanoparticles can effectively inhibit the transfer, see Figs. 8d and 9. The tribo-oxidation of agglomerated TiCN nanoparticles (20 wt % TiCN) can effectively reduce the friction coefficient. The role of tribo-oxidation should be clarified by revealing both the chemical composition and microstructure of the tribo-layer on the worn surface of Al_2O_3-Ti(CN) composites.

Lubricious oxide formed by tribo-oxidation of the second phase nanoparticles at high temperature proves to be effective for A10T and A20T composites. Lubricious double oxides can be generated on the fractional surface of Al_2O_3-based nanocomposites by using a third phase. Lubricious double oxides may provide good lubrication at a higher temperature or wider temperature range [9].

3.4 Conclusions

A concept for designing and fabricating high temperature self-lubricating Al_2O_3-based nanocomposites is proposed using Al_2O_3-Ti(CN) composites as an example. Al_2O_3-Ti(CN) composites with dispersed and agglomerated TiCN nanoparticles were successfully prepared by hot pressing at 1,400 °C. Al_2O_3-Ti(CN) composites with dispersed TiCN nanoparticles have high hardness and good resistance to abrasive wear at room temperature. Al_2O_3-Ti(CN) composites with dispersed (10 wt %) and agglomerated (20 wt %) TiCN nanoarticles are self-lubricating in sliding against Ni-Cr alloy at 500 °C.

Acknowledgments The authors acknowledge for the financial support from National Science Foundation of China (51075382) and One-hundred Talent Project (Junhu Meng) of Chinese Academy of Sciences.

References

1. Jahanmir S (1994) Friction and wear of ceramics. Marcel Dekker Inc, New York
2. Niihara K (1991) New design concept of structural ceramics-ceramic nanocomposite. J Ceram Soc Jpn 99:974–982
3. Sekino T et al (1997) Reduction and sintering of a nickel-dispersed-alumina composite and its properties. J Am Ceram Soc 80:1139–1148
4. Limpichaipanit A, Todd RI (2009) The relationship between microstructure, fracture and abrasive wear in Al_2O_3/SiC nanocomposites and microcomposites containing 5 and 10 % SiC. J Eur Ceram Soc 29:2841–2848
5. Ortiz-Merino JL, Todd RI (2005) Relationship between wear rate, surface pullout and microstructure during abrasive wear of alumina and alumina/SiC nanocomposites. Acta Mater 53:3345–3357
6. Shapiro IP et al (2011) An indentation model for erosive wear in Al_2O_3/SiC nanocomposites. J Eur Ceram Soc 31:85–95
7. Chen HJ et al (2000) The wear behaviour of Al_2O_3-SiC ceramic nanocomposites. Scripta Mater 42:555–560
8. Lu JJ et al. (2010) Friction and wear of Al_2O_3-Ni composite. In: Davim JP (ed) Tribology of composite materials. Nova Science Publishers Inc, New York
9. Erdemir A (2000) A crystal-chemical approach to lubrication by solid oxides. Tribol Lett 8:97–102